

Low noise optical receivers

Z. Bielecki¹, W. Kolosowski¹, R. Dufrene², M. Borejko³

¹ Military University of Technology, 2 Kaliskiego Str. 00-908 Warszawa, Poland, phone (+48 22) 683-97-89

² R. Dufrene. Telecommunications Research Institute. Warsaw, Poland

³ M. Borejko. Scientific Industrial Centre of Professional Electronics RADWAR, Warsaw, Poland

Abstract – the paper describes low noise first stage optical receivers. Analysis of operating conditions affecting signal-to-noise ratio has been carried out. Each preamplifier was carefully optimised to work with particular type of the detector.

Keywords – optical detectors, low noise preamplifier.

I. INTRODUCTION

Optical radiation receivers are used in many up-to-date fields of science and technology determining current level of technological progress. The most important fields of their applications are industrial automation, robotics, space technology, medicine, and military technology.

Photodetectors and low-noise signal processing are the main components of a receiver of optical radiation. Signal amplitude at the detector output is of very low value and in many cases is similar to noise level value. Thus, for signal amplification the low-noise systems should be used. Preamplifiers should ensure adequate amplification, their own noise should be low and their bandwidth should be broad enough to obtain non-distorted reproduction of a shape of input signals.

The noise produced in detectors and systems of signal processing circuits constrained detection of low intensity signals (Fig. 1).

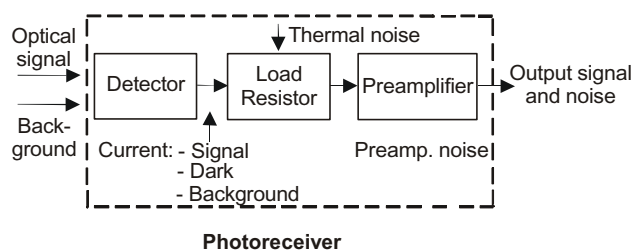


Fig. 1. Main noise sources in photoreceiver.

Optical radiation from an object is detected by a photoreceiver. Total radiation received from any object is the sum of the emitted, reflected and transmitted radiation [1,2]. Objects that are not blackbodies emit only fraction of blackbody radiation, and the remaining fraction is either transmitted or, for opaque objects, reflected. When the scene is composed of the objects and backgrounds of similar temperatures, the reflected radiation tends to reduce the available contrast. However, reflections of hotter or colder objects significantly effect the appearance of a thermal scene. The reflected sunlight is negligible for 8 – 14 μm imaging, but it is important in UV, VIS and 3-5 μm band [3].

An optical block in IR receiver produces an image of the observed objects in plane of the detector. The optical elements like windows, domes and filters can be used to protect the receiver from environment or to modify detector spectral response.

The most popular materials used for manufacturing of refractive optics of IR systems are: germanium (Ge), silicon (Si), fused silica (SiO_2), zinc selenide (ZnSe), glass BK-7, and zinc sulphide (ZnS).

Photons may originate from a variety of sources: scene background, path radiance, optics, warm filters, cold filter, and housing. The background noise can be reduced by using cold shield housing (Fig. 2). Photon noise is unique to thermal imaging systems. It is nonexistent for visible sensors since the background in the visible does not provide any photons. If the cold shield is isolated from the cooler, it may be at an elevated temperature. A warm filter (not shown) can also contribute to photon noise.

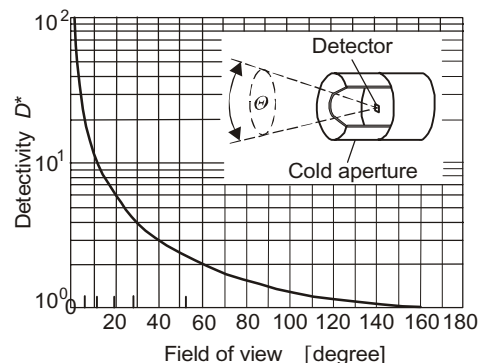


Fig. 2. Cold shield housing decreases photon noise.

There is no essential difference in design rules of optical objectives for visible and IR ranges. Designer of IR optics has significantly fewer materials suitable for IR optical elements, in comparison with those for visible range, particularly for wavelengths over 2.5 μm .

II. MAXIMISATION SIGNAL-TO-NOISE RATIO

Figure 1 shown a simple block diagram of the first stage of a photoreceiver (photodetector plus low noise preamplifier and biasing circuit of the detector). The optical signal and background radiation impinge on the photodetector inducing a current in the external load resistor. If P_λ is average optical power, then I_{ph} the average photocurrent, is given by

$$I_{ph} = \frac{\eta q P_{\lambda}}{h\nu} \cdot \quad (1)$$

where q is the electron charge, η is the quantum efficiency, h is the Planck constant and ν is the optical frequency of light.

To convert this to volts, simply multiply by the load resistor. For 100 % sinusoidal modulated signal, the rms optical power is given by $P_{\lambda}/\sqrt{2}$, and the rms photocurrent is

$$I_{ph} = \frac{\eta q P_{\lambda}}{\sqrt{2}h\nu} \cdot \quad (2)$$

Generation and recombination noise results from statistical fluctuation in the rate of generation and rate recombination of charged particles into an upper state within the detector material. The statistical fluctuation in the concentration of carriers produces the white noise, which has electrical frequencies less than the inverse of carrier lifetime. The current noise generated and recombined in the bulk before reaching electrodes. The current noise expression for generation-recombination noise is

$$I_{G-R} = 4q^2\eta(\Phi_s + \Phi_b)Ag^2\Delta f + 4q^2G_{th}g^2\Delta f, \quad (3)$$

where Φ_s is the radiant incident power from the signal, Φ_b is the radiant incident power from the background, A is the detector area, g is the photoconductive gain, Δf is the electronic frequency bandwidth, G_{th} is the thermal conductance.

Johnson noise of the detector (R_d) and load resistance (R_L) is the fluctuation caused by the thermal motion of the charge carriers in resistive element. The Johnson noise current of the detector and load resistance R_L is given respectively

$$I_{J-d} = \frac{4kT_d\Delta f}{R_d} \quad \text{and} \quad I_{J-L} = \frac{4kT_L\Delta f}{R_L}, \quad (4)$$

where T_d is the detector temperature, R_d is the detector resistance, T_L is the load resistance temperature.

Shot noise is associated with the dc current flowing across a potential barrier and is a series of independent events. Because the dc current is proportional to the cross-sectional area of the detector, this noise is also proportional to the square root of the detector area, if the potential barrier cross-sectional area is the optical active area, as is typical for a photodiode. The current-noise expression for shot noise is

$$I_{sh} = (2qI\Delta f)^{1/2}. \quad (5)$$

If I is the result of photons, that is, a photocurrent, then the noise of the detector is photon-noise limited.

$1/f$ noise is a strong function of frequency, and most important at low audio frequencies. The noise power is approximately inversely proportional to the frequency

$$I_{1/f} = \frac{kI_b^\alpha}{f^\beta}, \quad (6)$$

where k is the Boltzmann constant, I_b is the bias of the detector, f is the electrical frequency.

The one-over- f noise magnitude is affected by nonohmic contacts at electrodes, and surface-state traps that cause current flow to be interrupted by variations in the trapping time constant. One-over- f noise is always

present in both photoconductors and bolometers, because there is always a dc-bias current present.

The main purpose was to analyse the input stages of photoreceivers to optimise them providing maximal value of signal-to-noise ratio.

A general noise model of the detector and load circuit has been accepted (Fig. 3).

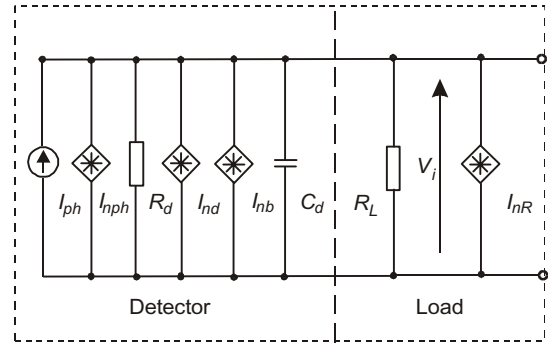


Fig. 3. Equivalent noise model of a detector and load of the photoreceiver.

(where I_{ph} is the photocurrent, I_{nd} is the detector noise, I_{nb} is the background noise, C_d , R_d are the capacity and resistance of a detector respectively).

Preamplifiers used for photoreceivers can be classified as three categories: low impedance preamplifiers, high impedance preamplifiers and transimpedance preamplifiers. The active device of a preamplifier can be bipolar, JFET, or it can be an IC with bipolar, FET or MOSFET input stage

Selection of active device primarily depends on detector resistance and frequency range. It is difficult to say exactly where device of each type should be used. The input active device of the preamplifier, is usually the dominant noise contributor of the readout. The noise contribution of the input transistor is a function of the source impedance exhibited by the detector. Thus, it is important to match the detector with an appropriate readout input transistor [4].

Preamplifier noise is presented as two sources, voltage and current ones. Basing on the analysis of noise models of the receivers with photoconductive detectors, the following expression for S/N ratio can be written [5]

$$\frac{S}{N} = \frac{I_{ph}^2}{I_{1/f}^2 + I_{G-R}^2 + I_{J-d}^2 + I_{J-L}^2 + I_a^2} \quad (7)$$

where I_a is the preamplifier noise.

The counter exhibits the squared average value of a photocurrent and the dominator shows the total equivalent input noise. The first term of the denominator determines the noise of $1/f$ type, the second one - generation-recombination noise resulted from fluctuations of radiation from signal and background, the third term - generation-recombination noise produced by thermally excited carriers in semiconductors, next terms represent thermal noise of detector resistance, loading, and preamplifier.

The noise of $1/f$ type depends on technology of detector manufacturing and the value of a bias current.

The second term can be reduced due to narrowing the detector's field of view, application of cooled diaphragms and optical filters. Lowering the detector temperature causes reduction of the third and fourth terms. High load resistance gives thermal noise minimisation. The optimised preamplifiers of low noise should be used.

To analysis of S/N ratio of the receivers with photodiode, the following expression for S/N ratio was obtained [5]

$$\frac{S}{N} = \frac{M^2 I_{ph}^2}{2q\Delta f \left[(I_{ph} + I_b) M^2 F + (I_s + I_{db} M^2 F) 2 \frac{T-300}{10} \right] + \frac{4kT\Delta f}{R_L} F_n} \quad (8)$$

where M is the multiplication factor, F is the photodiode noise factor, V is the bias voltage of the photodiode, and F_n is the noise factor of the preamplifier.

The counter includes squared average value of photocurrent multiplied by squared multiplication factor of an avalanche photodiode. Denominator represents the total substitute input noise of a receiver. The first term of Eq. (8) describes shot noise, the second one - thermal noise of load resistance and preamplifier noise. Shot noise depends on photocurrent, background current, as well as on superficial and volumetric components of dark current.

The results of the above mentioned activities were used for experimental investigations, i.e., several IR detection devices were designed, performed, and tested [6-8].

III. EXAMPLES OF PREAMPLIFIER AND EXPERIMENTAL RESULTS

Many problems have to be overcome during construction of low-noise preamplifier for low-resistance detectors (e.g., HgCdTe of resistance below 100 Ω). It is due to the fact that the detectors of resistance of the order of 20 Ω produce noise voltage lower than 0.6 nV/Hz^{1/2}, i.e., below the noise voltage generated in the best (available) amplifying elements [9]. So, the question arises; it is possible to build a preamplifier of noise voltage below a detector noise? It appears that it can be achieved when several identical preamplifiers are connected in parallel and next the output signals are added.

Such a system of signal processing ensures reduction of final input signal according to the relationship

$$V_{n\ total} = V_n \cdot (n)^{-1/2}, \quad (9)$$

where V_n is the noise voltage of a single preamplifier and n is the number of amplifying stages.

Figure 4 presents a diagram of transimpedance preamplifier that is recommended for amplification of the signals received from low-resistance IR detectors. Low noise transistors MAT 03 type were used at the input stage of an preamplifier. This preamplifier can be applied both for photodiodes and photoresistors. When a photoresistor is connected, the polarising resistor R_L is required.

For this system the noise voltage was 0.35 nV/Hz^{1/2} at $f = 10$ kHz.

For amplification of the signals from detectors of resistances of above 10 M Ω , the most frequently used are voltage and transimpedance amplifiers. The basic idea of increase in input impedance of preamplifier is reduction of thermal noises. However, the high resistances R_L cause narrowing of a band of the input stage of a photoreceiver.

A preamplifier of high input impedance is significant load resistance for a detector so, it does not ensure wide range of signal changes. The problem of serious changes of a signal has been solved in transimpedance preamplifiers.

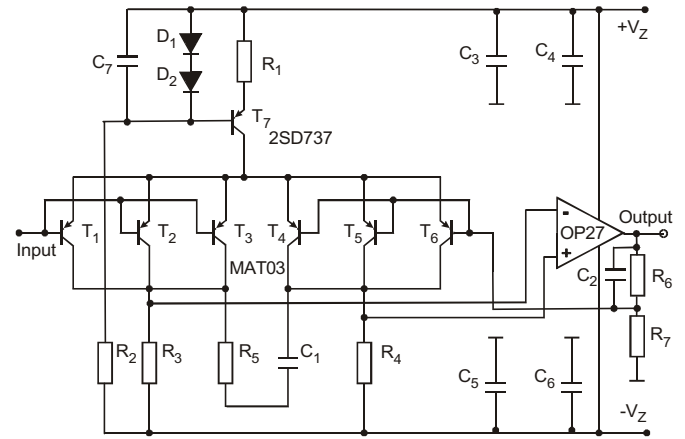


Fig. 4. Preamplifier for low-resistance infrared detectors.

For amplification of the signals from high-resistance detectors, the system was used the simplified scheme of which is shown in Fig. 5.

In the preamplifier, the integrated circuit of OPA 129 type was used.

The output voltage to the op-amp is then

$$V_{in} = I_{ph} Z_d, \quad (10)$$

where Z_d is the detector impedance.

The detector impedance is given by

$$Z_d = \frac{R_d}{1 + j\omega R_d C_d}. \quad (11)$$

Since the feedback impedance and detector impedance act as a voltage divider between V_{out} and ground, and since we can assume that $V_{in} \ll V_{out}$, the output voltage is

$$V_{out} = -V_{in} \frac{Z_f}{Z_d}, \quad (12)$$

where

$$Z_f = \frac{R_f}{1 + j\omega R_f C_f}. \quad (13)$$

From equation 10 and 13 we obtain

$$V_{out} = -\frac{I_{ph} R_f}{1 + j\omega R_f C_f}. \quad (14)$$

The amplitude of V_{out} is its absolute value,

$$|V_{out}| = (V_{out}^* V_{out})^{1/2} = \frac{|I_{ph}| R_f}{(1 + \omega^2 \tau_f^2)^{1/2}}, \quad (15)$$

where $\tau_f = R_f C_f$.

The signal and cutoff frequency f_f is the frequency at which the signal has decreased by a factor of $\sqrt{2}$

$$f_f = \frac{1}{2\pi R_f C_f} = \frac{1}{2\pi \tau_f}. \quad (16)$$

Notice that the output voltage is independent of R_d and C_d . As long as R_f is linear and I_{ph} is a linear function of the photon flux, the detector-amplifier system is linear. Moreover, even if $R_d C_d \gg \tau_f$, the frequency response of the system is determined by τ_f , the limit imposed by the feedback resistor. As the detector impedance decreases with increasing frequency, the transimpedance gain increases to compensate (equation 12). The high frequency performance is improved substantially for photodiodes because the capacitance of the feedback resistor can be made much smaller than that of the detector.

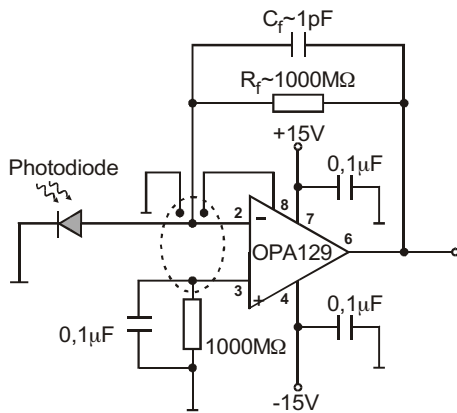


Fig. 5. Preamplifier for high-resistance infrared detectors.

The noise analysis of the preamplifier was also performed by mean of the computer programme CLIENT 99 of the Protel International PLD Ltd. Firm. The programme ensures determination of approximate noise parameters already at the stage of a system design. It is especially important for design of low-noise amplifiers used in measuring or detecting systems of very low signals. Thus, due to computer simulation we can avoid designing the input stages of measuring or detecting systems, that do not fulfil the assumed requirements.

Next, we have measured noise level of a preamplifier using the method presented in Fig. 6.

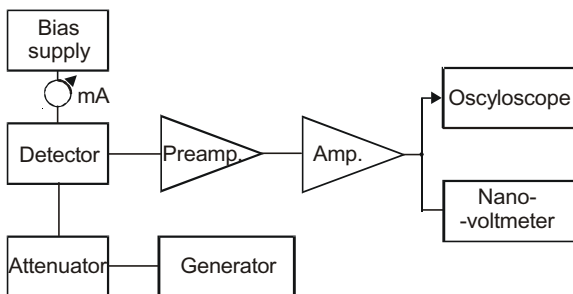


Fig. 6. Noise measurement system.

This is a measurement system recommended by MIL-STD-202 standard. Noise was measured using homodyne nanovoltmeter SR 830 DSP type. The received input noise current was $0.25 \text{ fA/Hz}^{1/2}$ for $f = 10 \text{ kHz}$. Measurement noise is about 1.4 times higher than the calculated one.

Further works on improvement in preamplifiers for low-resistance HgCdTe and GaN detectors are being made.

IV CONCLUSION

Research and design works were limited to the signal processing systems employing photovoltaic infrared detectors. An analysis of noise models of photodetector preamplifier systems was carried out. The preamplifiers are designed for detectors. Each preamplifier is carefully optimised to work with particular type of the detector. Current mode configuration results in excellent stability of the first stage in all working conditions. Special attention has been paid to ensure maximum signal to noise ratio in wide range of detectors resistance. All input stages of the AC preamplifiers employ ultra low noise transistors so the bias point can be precisely trimmed to obtain the optimal matching with the detector. The models of preamplifiers are placed in integrated housing which provides for the thermoelectric cooler of the detector, effective EMI shielding, and is more convenient for customer. Our preamplifiers are individually optimised to work with optical detectors. However, they can be used with many types of detectors commercially available.

The elaborated preamplifiers can be used in IR pyrometers, IR sensors, thermal scanners, IR thermal cameras, smart munitions, and in many other applications.

REFERENCES

- [1]. A. Rogalski and J. Piotrowski, "Intrinsic infrared photodetectors," *Prog. in Quant. Electr.* **12**, 1988.
- [2]. G.H. Rieke, *Detection of Light: from the Ultraviolet to the Submillimeter*, Cambridge, Cambridge University Press, 1994.
- [3]. C.T. Elliot, D. Day, and D.J. Wilson, "An integrating detector for serial scan thermal imaging," *Infrared Phys.* **22**, 31–42 (1982).
- [4]. C.D. Mothenbacher, J.A. Connelly. *Low-noise electronic system design*. New York, Wiley 1995.
- [5]. Z. Bielecki, "Maximisation of signal to noise ratio in infrared radiation receivers," *Opto-electron. Rev.* **10**, 209–216 (2002).
- [6]. Z. Bielecki. "Photoreceiver with avalanche C-30645 photodiode" *IEE Proceedings Optoelectronics*, **147**, 234–236 (2000).
- [7]. Z. Bielecki, "Photoreceiver with popcorn-noise reduction systems," *26th International Conference on Infrared and Millimeter Waves*, 10–14 September, Toulouse, France, 72–73 (2001).
- [8]. Z. Bielecki, "Elimination of popcorn noise in receivers with pyroelectric detectors". *International Conference Infrared Sensors & Systems*, Erfurt, *Proc. IRS²*, 173–177 (2002).
- [9]. Catalog Rohm Co. Ltd. *Epitaxial planar npn silicon transistors 2SD 786 type* (1990).